

Reactivity of Nickel-Titanium with Methanolic Bromine and Iodine Solutions. Etching Characteristics of a Shape-Memory Alloy

Kathleen R. C. Gisser, Dean M. Philipp, and Arthur B. Ellis*

Department of Chemistry, University of Wisconsin—Madison, Madison, Wisconsin 53706

Received February 26, 1992

Nickel-titanium (NiTi) alloys having composition $\text{Ni}_x\text{Ti}_{1-x}$ ($0.47 \leq x \leq 0.51$) exhibit a martensitic transformation that gives rise to a shape-memory effect near room temperature. Normally chemically inert, these alloys react with wet methanolic Br_2 and I_2 solutions to yield crystalline nickel halides and uncharacterized titanium-containing products. The crystalline products are independent of whether NiTi is in its high-temperature (austenite) or low-temperature (martensite) phase. Reaction rates were measured for austenitic NiTi: concentrated Br_2/MeOH solutions corrode the surface at room temperature at a rate of up to 2000 Å/s; solutions of I_2/MeOH reach a decomposition rate of only ~5 Å/s. For the Br_2/MeOH reaction, kinetic studies were conducted with samples of pure martensite, pure austenite, or mixtures of these phases. An average apparent activation energy of 13.4 ± 1.6 kJ/mol was obtained irrespective of the NiTi phase(s) present. At concentrations exceeding ~3 M Br_2 in MeOH, the reaction with NiTi polishes the surface of the bulk alloy, yielding features on the order of ~1 μm; at low concentrations, visibly textured surfaces are created.

Introduction

Nickel-titanium (NiTi) is one of a family of materials known as shape-memory alloys (SMAs). Alloys with composition $\text{Ni}_x\text{Ti}_{1-x}$ ($0.47 \leq x \leq 0.51$) are prepared for use in a variety of commercial applications by first annealing them into a particular shape at ~500 °C. If the alloy is deformed at or slightly below room temperature, modest heating to between 0 and 80 °C, the exact temperature depending on sample composition, will return the sample to its original, annealed shape.^{1,2}

The ability to "remember" the annealed shape is the result of a solid-state phase transformation. The nickel-to-titanium ratio tunes the temperatures at which the high-temperature austenite phase, which has the CsCl structure, and the low-temperature martensite phase, which has a monoclinic structure, interconvert. The transitions into the high-temperature phase and into the low-temperature phase do not occur at the same temperature: There is a hysteresis loop, shown in the idealized sketch of Figure 1, associated with the phase change that has been probed by X-ray diffraction,³ calorimetry,⁴ electrical conductivity,⁵ and magnetic susceptibility⁶ measurements. The phase transformation is characterized by temperatures corresponding to the start and finish of the transformation into the austenite, A_s and A_f ; and by temperatures corresponding to the start and finish of the transformation into the martensite, M_s and M_f . The width of the hysteresis loop is typically 20–50 °C.

Alloys of NiTi are generally unreactive, accounting for their use in orthodontic and medical applications that require biocompatibility.⁷ To our knowledge, reactivity studies have been limited to highly concentrated ionic solutions and solutions mimicking physiological conditions.^{8–10} Given the potential need for controlled etching and polishing of NiTi for use in thin-film-based actuators and micromachines, we sought to find and characterize reagents that could be used for such purposes.

We report herein that wet methanolic solutions of Br_2 and I_2 react with bulk, polycrystalline NiTi in either the austenite or martensite phase to yield nickel halides and uncharacterized titanium-containing products. Corrosion rates at room temperature of up to ~2000 Å/s can be

Table I. Transition Temperatures for NiTi Samples^a

sample	M_f^b	M_s^c	A_s^d	A_f^e
A		<6	6	20
B		<18	18	40
C	20'	30'	50	70

^a Transition temperatures for the phase changes in °C, as determined by differential scanning calorimetry, provided by U.S. Nitinol except where noted. ^b Temperature at which conversion to the martensite phase, induced by cooling, is complete. ^c Temperature at which conversion to the martensite phase, induced by cooling, begins. ^d Temperature at which conversion to the austenite phase, induced by heating, begins. ^e Temperature at which conversion to the austenite phase, induced by heating, is complete. ^f Transition temperature was determined by electrical resistance measurements provided by TiNi Alloy Co.

achieved with concentrated Br_2/MeOH solutions, and apparent activation energies for this reaction have been determined for both phases of the NiTi starting material. Moreover, a range of surface textures can be produced by the reaction, from highly pitted at low halogen concentration, to highly polished at high halogen concentration.

Experimental Section

Materials. Unless otherwise specified, all experiments on NiTi were performed on bulk samples obtained from U.S. Nitinol, Saratoga, CA. Disks from three lots, with A_s temperatures of 6, 18, and 50 °C were used and are referred to herein as samples A, B, and C, respectively. All of the characterized transition

(1) Collen, K. R.; Ellis, A. B.; Perepezko, J. H.; Moberly, W.; Busch, J. D. In *Chemistry of New Materials*; Rao, C. N. R., Ed.; Blackwell: Oxford, in press.

(2) Perkins, J. *Met. Forum* 1981, 4, 153.

(3) Michal, G. M.; Sinclair, R. *Acta Crystallogr. Sect. B* 1981, 37, 1803.

(4) Airoldi, G.; Riva, G.; Rivolta, B. *MRS International Mtg. on Adv. Mats.*; Doyama, M.; Somya, S.; Chang, R. P. H., Eds.; MRS: Pittsburgh, 1989; Vol. 9, p 105.

(5) Wayman, C. M.; Cornelis, I. *Scr. Met.* 1972, 6, 115.

(6) Wasilewski, R. J.; Butler, S. R.; Hanlor, J. E. *Met. Sci. J.* 1967, 1, 104.

(7) Liu, X.; Stice, J. *J. Appl. Manuf. Syst.* 1990, Jan, 65.

(8) Rondelli, G.; Vicentini, B.; Cigada, A. *Corrosion Sci.* 1990, 30, 805.

(9) Liu, S. In *Engineering Aspects of Shape Memory Alloys*; Duerig, T. W., Ed.; Butterworths: London, 1990.

(10) Sekiguchi, Y. In *Shape Memory Alloys*; Funakubo, H., Ed.; Gordon and Breach: New York, 1984.

* To whom correspondence should be addressed.

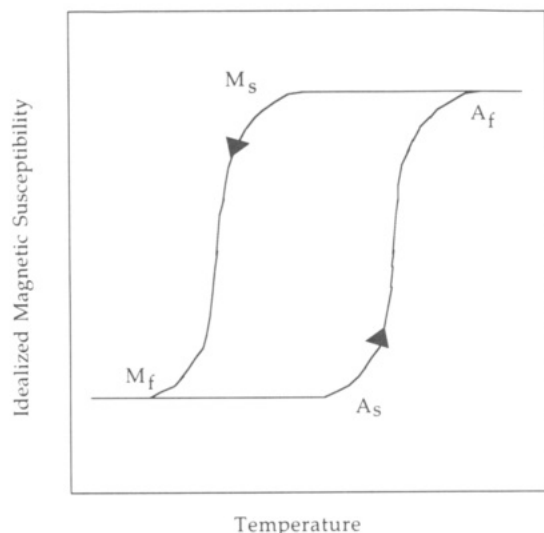


Figure 1. Hysteresis loop associated with the NiTi phase change. In this figure, changes in the idealized magnetic susceptibility are shown as a function of temperature in the phase transformation regime. There are two sets of transition temperatures: A_s and A_f (the start and end of the transition into the austenite), and M_s and M_f (the start and end of the transformation into the martensite).

temperatures for these samples are collected in Table I. The disks were cut into blocks, $\sim 1.0 \times 1.0 \times 0.5 \text{ cm}^3$. The following reagent grade compounds were used without further purification: iodine and MeOH (Mallinckrodt); bromine, KMnO_4 , and HI (Fisher); HBr and $\text{K}_2\text{Cr}_2\text{O}_7$ (Matheson); Ni powder, 99.9% (Ceraac); Ti wire, 99.99%, and CCl_4 (Aldrich); NiTi wire, 99% (TiNi Alloy Co., Oakland, CA); ether (Columbus); HNO_3 (EM).

Equipment. X-ray diffraction (XRD) powder patterns were taken on a Nicolet R3m/V polycrystalline X-ray diffraction system (Cu $K\alpha$ radiation). Auger electron spectroscopy (AES) measurements and secondary electron micrographs were taken with a Perkin-Elmer Model 660 scanning Auger multiprobe; Ar^+ sputter etching provided a depth profile of the NiTi. A Bransonic B-220 ultrasonic cleaner was used to prepare NiTi samples for introduction into the Auger spectrometer. Proton NMR spectra were taken using a Bruker 200-MHz spectrometer.

Before reaction, the NiTi was sanded with a Zero Blast-N-Peen bead-blast to ensure that any previously reacted surface was removed. All sample weights were measured to $\pm 10 \mu\text{g}$ with a Sartorius balance, and the dimensions of the NiTi samples were measured to $\pm 0.01 \text{ mm}$ with a Max-Cal electronic digital caliper. Temperature control of the reaction cell was maintained at $\pm 0.5^\circ\text{C}$ with a Precision Scientific Group R20 constant-temperature bath. When necessary, sample preheating was done in a Lindberg Heavy Duty 4838-101 tube furnace, controlled to $\pm 1^\circ\text{C}$ by a Eurotherm 812 controller/programmer.

Identification of Reaction Products. NiTi wire was reacted to completion with a stoichiometric excess of bromine and iodine in wet methanol in order to determine reaction products. The resulting solutions were dried under vacuum until only a solid residue remained. In the iodine case, the product was also sublimed to remove any excess iodine. The X-ray powder diffraction patterns of the residue were then taken. The same procedure was followed with nickel powder and titanium wire as reactants. Elemental analysis of the Ti/bromine product (Galbraith) yielded the following composition: C, 10.04%; H, 4.04%; Ti, 17.33%; Br, 40.07%; O, 28.52% (by subtraction).

Kinetic Measurements. Reaction rates for NiTi were measured using the following procedure, hereafter referred to as the "standard method": A block of NiTi was cleaned using the bead blaster and pretreated in the reactant solution for two 30-s intervals. The NiTi was then measured with a caliper and weighed. The NiTi weight loss was measured as a function of time by immersing the sample in the reactant solution for 30 s, removing it, rinsing it in methanol, and drying it under a stream of compressed air. In a small number of trials, an opaque film of unknown origin grew on the sample, halting the reaction. In these

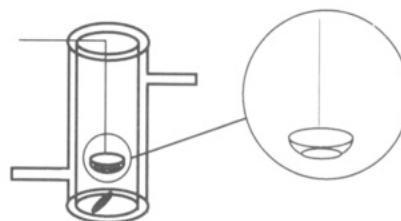


Figure 2. Thermostatic reaction cell. Ethanol is pumped through the inlet and outlet arms of the glass reaction cell. The sample holder, shown at the right, has a low lip and a hole in the bottom to ensure that all sides of the sample are exposed to the reactant solution. A magnetic stir bar is shown at the bottom of the cell.

cases the sample was recleaned in the bead blaster, and the data were disregarded.

The kinetic measurements were carried out in the cell shown in Figure 2. The double-walled glass cell was used to maintain the temperature of the reactant solutions. A thermostatic water/ethanol bath was pumped through the outer wall of the cell. The temperature of the reactant solution was monitored by a mercury thermometer. The NiTi sample was raised and lowered into the cell with a glass holder. The holder was spoon-shaped, with a low lip, and a large hole in the bottom to expose all six faces of the NiTi sample to the reactant solution (see inset, Figure 2).

Relative Reactivity Studies. The reaction rate of NiTi in the austenite phase (sample A; $A_s = 6^\circ\text{C}$, $A_f = 20^\circ\text{C}$) was measured with several potential reactants by the standard method at room temperature. Reactant solutions of Br_2 , I_2 , HI, and HBr, each 1 M in methanol, were used. (The concentrations of these solutions were limited by the maximum solubility of I_2 in MeOH, which is about 1.3 M.) Addition of KI to a saturated I_2/MeOH solution with a small excess of solid I_2 did not cause the excess I_2 to dissolve. Proton NMR spectra of MeOH and the two halogen/MeOH solutions were taken after standing for 2 h at room temperature. All three solutions showed the same peaks at $\delta = 3.46$ and 7.42 , indicating that the halogens did not react with the solvent. Since reactant concentrations of 1.0 M degrade the surface finish (vide infra), initial rates were used to compare the relative reactivities.

Exposing NiTi to concentrated acidic solutions of $\text{K}_2\text{Cr}_2\text{O}_7$ and KMnO_4 in water did not result in any observable reaction. The reaction of NiTi with 2.0 M solutions of bromine in CCl_4 or ether, and with saturated solutions of bromine in water was much slower (by at least a factor of 10) than in methanol.

Temperature Dependence of Reactivity. The temperature dependence of the reaction rate was measured in 3.9 M (20% v/v) Br_2/MeOH solutions; slight (25%) reductions in the bromine concentration and stirring rate did not affect the measured reaction rate. NiTi in the austenite phase (sample A; $A_s = 6^\circ\text{C}$, $A_f = 20^\circ\text{C}$) was reacted at temperatures between 20 and 60°C . Corrosion rates were calculated from the measured weight losses. The apparent activation energy was extracted from a plot of \ln (relative corrosion rate) vs reciprocal temperature.

Phase-Dependent Reactivity. The effect of the initial NiTi crystal structure on the reaction was measured in two ways: by directly comparing the reaction rate of the same sample in two different phases at the same temperature, and by comparing the activation energies of the reaction performed on the austenite and martensite phases.

(i) **Direct Comparison of Reaction Rates.** The reaction rate with 3.9 M Br_2/MeOH was measured for sample C ($A_s = 50^\circ\text{C}$, $A_f = 70^\circ\text{C}$) in both the austenite and martensite phases. The M_s and M_f temperatures for this sample were 30 and 20°C , respectively, determined by four-probe resistance measurements (TiNi Alloy Co., Oakland, CA). The reaction rate of this sample with bromine was measured twice at 40°C , once after heating it into the austenite phase in a tube furnace at 70°C and again after cooling it in air over dry ice (-10 to -15°C) into the martensite phase.

(ii) **Comparison of Apparent Activation Energies.** The apparent activation energy of the NiTi/ Br_2 reaction was also determined as a function of the phase of the NiTi. Reaction rates for all three samples were used in order to compare particular

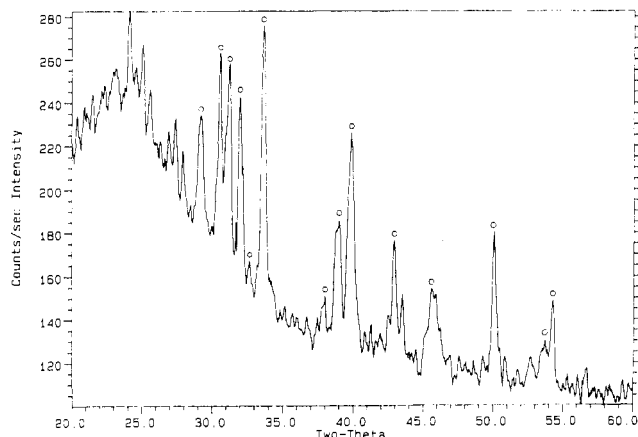


Figure 3. Powder X-ray diffraction pattern of the reaction products of NiTi with methanolic bromine. Peaks marked O correspond to $\text{NiBr}_2 \cdot 2\text{H}_2\text{O}$.

phases over a range of temperatures.

(a) *Apparent activation energy of the austenite/bromine reaction:* The apparent activation energy of the Br_2 reaction was measured using the standard procedure described above. To probe only the austenite phase, the NiTi blocks were heated in a tube furnace before each 30-s immersion in the bromine solution. To ensure that the preheating did not artificially accelerate the reaction, the samples were allowed to equilibrate in a furnace at the reaction temperature. The reaction rate was measured at temperatures between 20 and 60 °C after preheating. Since $M_s < A_s$, samples A and B ($A_s = 6$ and 18 °C) were in the austenite phase over the entire 20–60 °C range. Sample C ($M_s = 30$ °C) was also in the austenite phase except for trials at 20 °C, which were disregarded for the analysis.

(b) *Apparent activation energy of the martensite/bromine reaction:* NiTi samples were cooled over dry ice in order to transform them into the martensite phase. However, when they were equilibrated in the 20–60 °C range (to obtain data in 10 °C increments) before the reaction, they did not necessarily remain in the martensite. Sample A ($A_s = 6$ °C, $A_f = 20$ °C) converts back to the austenite, and sample B ($A_s = 18$ °C, $A_f = 40$ °C) is in the martensite phase for the lower temperatures but converts to the austenite as trials are taken at higher temperatures. Sample C ($A_s = 50$ °C) may be reacted in the martensite phase except at 60 °C.

Surface Morphology. The effects of reactant concentration on the surface finish of the NiTi were determined by reacting NiTi according to the standard method in solutions of 0.97, 1.9, 2.9, and 3.9 M (5, 10, 15, and 20 vol %) bromine in MeOH. These samples were allowed to react continuously for 5 min, at which point the surface relief on the samples reacted at lower bromine concentration was easily visible to the naked eye. The samples were washed in MeOH, sonicated for 15 min in MeOH, and allowed to dry overnight before introduction into the Auger vacuum chamber. Secondary electron micrographs were taken at 1000× with a 5-kV beam voltage.

Results and Discussion

Reactivity of NiTi. Nickel–titanium, like most titanium alloys, is extremely inert due to an impervious oxide coating. However, we find that concentrated methanolic solutions of bromine and iodine are capable of reacting with NiTi. Powder XRD of the products of the NiTi reaction with bromine (Figure 3) show a diffraction pattern that matches that of $\text{NiBr}_2 \cdot 2\text{H}_2\text{O}$, as well as a large number of other peaks. These peaks could not be identified as TiBr_2 , TiBr_3 , TiBr_4 ,¹¹ $\text{Ti}(\text{OMe})_4$,¹² $[\text{Ti}_4\text{O}_6(\text{H}_2\text{O})_{12}]\text{Br}_4$,¹³ or

any of the reported TiO_2 or TiO phases.

To identify the titanium product, reactions of the individual metals were run. Reaction of nickel alone with bromine produces $\text{NiBr}_2 \cdot 2\text{H}_2\text{O}$,¹⁴ in very large yields (>90%). However, reaction of titanium with methanolic bromine solutions resulted in viscous orange-yellow solution from which we were not able to crystallize a product. Elemental analysis of the Ti/bromine product did not correspond to any of the titanium phases cited above.

The reaction of nickel with I_2 is a standard preparation for NiI_2 ,¹⁵ and this phase may be easily identified in the powder pattern for the vacuum-dried products of the NiTi reaction with iodine; on standing in air, the NiI_2 hydrates to form $\text{NiI}_2 \cdot 6\text{H}_2\text{O}$.¹⁶ As with the bromine case, we were unable to separately crystallize a titanium product from the reaction of NiTi with I_2 .

The solvent and reaction conditions strongly influence the reaction rate. At high concentrations, bromine reacts quickly with NiTi. However, when the NiTi/bromine reaction was run under comparable conditions in other good bromine solvents, CCl_4 and ether, the reaction proceeded slowly. One of the products in the bromine reaction, a hydrated nickel salt, demonstrates the involvement of water in the reaction, although the reaction in water is also slower than in methanol, possibly due to the limited solubility of bromine. Other strong oxidizing reagents were also tested, including acidic solutions of $\text{K}_2\text{Cr}_2\text{O}_7$ and KMnO_4 . However, no reaction occurred, underscoring the role of product formation in driving the reaction.

The NiTi crystal structure does not appear to have a significant effect on the net reaction chemistry. One sample of C was heated into the austenite phase ($A_s = 50$ °C, $A_f = 70$ °C) and another cooled into the martensite phase ($M_s = 30$ °C, $M_f = 20$ °C), and then both were equilibrated at 40 °C, in the middle of the hysteresis loop. X-ray powder diffraction verified that preheating or precooling sample C sets the desired phase. When the heated and cooled samples were reacted at 40 °C to completion in bromine, and the products dried under vacuum, the same X-ray powder pattern was obtained for the products from both the austenite and martensite starting materials.

Relative Reaction Rates. The reaction rates for NiTi with Br_2 and I_2 were determined at room temperature (25 °C) for samples in the austenite phase ($A_s = 6$ °C, $A_f = 20$ °C). Methanolic solutions of HI and HBr were also used for comparison. Since I_2 is much less soluble in MeOH than Br_2 , the concentration of the reagents was 1.0 M, which is nearly the concentration of a saturated iodine solution.

The reaction rates were measured by dipping the NiTi into the reaction solutions for 30-s intervals and weighing the sample after each interval. Initial rates were used for the comparison because the NiTi surface became rougher during the reaction. The change in weight was converted to a corrosion rate in Å/s, using the density of NiTi, 6.45 g/cm³,¹⁷ and the measured surface area.

Neither the HI nor the HBr appeared to react with the NiTi over a period of 30 min, in keeping with other reports

(13) Walter-Levy, L.; Ferey, G.; Iqbal, S. J. *C.R. Acad. Sc. Paris* 1967, 256, 700. A recent structure of the chloride analog of this compound may be found in: Reichmann, M. G.; Hollander, F. J.; Bell, A. T. *Acta Crystallogr., Sect. C* 1987, 43, 1987.

(14) JCPDS file 15-559 was used to identify $\text{NiBr}_2 \cdot 2\text{H}_2\text{O}$.

(15) Cotton, F. A.; Wilkinson, G. *Advanced Inorganic Chemistry*, 5th ed.; Wiley: New York, 1988; p 743.

(16) JCPDS file 16-565 was used to identify $\text{NiI}_2 \cdot 6\text{H}_2\text{O}$.

(17) Jackson, C. M.; Wagner, H. J.; Wasilewski, R. J. *NASA SP-5110, 55 Nitinol, the Alloy with a Memory*; NASA: Washington, DC, 1972; p 23. The difference in density between the two phases is less than 0.5%.

(11) JCPDS files 14-642, 12-611, and 11-64, were used to match TiBr_2 , TiBr_3 , and TiBr_4 , respectively.

(12) Wright, D. A.; Williams, D. A. *Acta Crystallogr. Sect. B* 1968, 24, 1107.

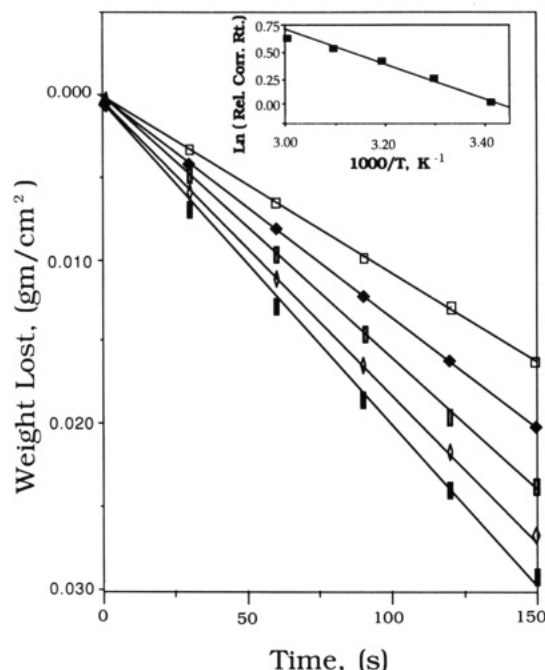


Figure 4. Typical kinetic data for the NiTi reaction (sample A; $A_s = 6$ °C, $A_t = 20$ °C) with 3.9 M methanolic bromine obtained at 20 (□), 30 (♦), 40 (○), 50 (△), and 60 °C, (●), and normalized for apparent surface area. The inset presents a semilog plot of the relative corrosion rates (relative to the rate at 20 °C, and taken from the slopes of the curves shown) vs reciprocal temperature. Over the temperature range studied, the slope of the Arrhenius plot yields an apparent activation energy of 13.2 ± 0.5 kJ/mol.

of the lack of reactivity of NiTi in the presence of most acids.¹⁸ In contrast, the I_2 /MeOH solution corroded the NiTi surface at a rate of ~ 5 Å/s, and the Br_2 /MeOH solution corroded the surface at a rate of ~ 2000 Å/s. Since the surface oxide on NiTi is typically 200–300 Å thick, this rate, measured over several minutes, results primarily from reaction of Br_2 with the metal itself, not the oxide. This substantial rate of reaction of NiTi with bromine is comparable to the 400 Å/s rates achieved with concentrated, room-temperature, aqueous HF/HNO₃ solutions that are commonly used to etch NiTi.¹⁹

Temperature Dependence of Reactivity. Although it was not possible to further concentrate the I_2 /MeOH solution, it was possible to raise the Br_2 concentration until the rate of the reaction was not mass-transport limited (3.9 M). As expected for a zeroth-order reaction, the measured weight loss was extremely linear over several minutes of testing. In this concentration regime, the reaction rate for the austenite phase was measured between 20 and 60 °C (Figure 4). At 20 °C, the corrosion rate was 1600 Å/s, and at 60 °C, the rate rose to 3000 Å/s. At temperatures over 60 °C, the bromine/MeOH solution evaporated so quickly that measurements were unreliable. In calculating the corrosion rates, the surface area was uncorrected for surface roughness; the samples reacted in 3.9 M (20%, v/v) bromine solutions were generally quite smooth (vide infra).

The kinetic data may be analyzed using an Arrhenius model, as shown in Figure 4, where the ln (relative corrosion rate) is plotted against reciprocal temperature. The apparent activation energy for sample A, extracted from the slope, is 13.2 ± 0.5 kJ/mol. This is extremely small, on the order of the energy needed to rotate about the single

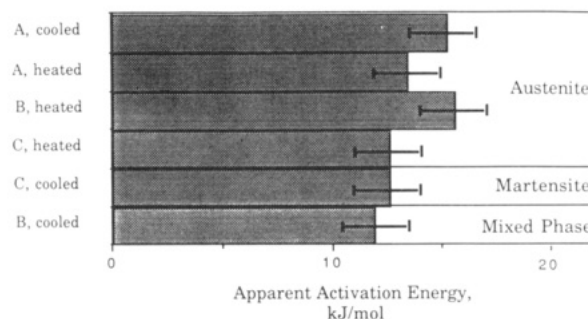


Figure 5. Apparent activation energies for samples in the austenite phase compared to those for martensitic and mixed phase samples. The apparent activation energies were extracted from Arrhenius plots (Figure 4 shows the data used to obtain the value for "A, heated" in this figure) for four austenitic samples, one martensitic sample, and one mixed-phase sample. The error bars represent the standard deviation in the slope of the Arrhenius plot for each type of sample. Since the values for the austenite phase span a range from 12 to 16 kJ/mol, the apparent activation energies for the reaction with the two phases are experimentally indistinguishable. The average apparent activation energy for the reaction, including values for all six samples, is 13.4 ± 1.6 kJ/mol.

bond in ethane.²⁰ Since the reaction is heterogeneous and extremely exothermic (a wire in the martensite can heat up enough to return to its austenitic shape if the solution is not stirred), the apparent activation energy cannot be ascribed to a particular rate-limiting step.

Phase Dependence of the Reactivity. Once the independence of the reaction products on the NiTi phase was established, differences in the reaction rate and activation energy were probed for the austenite and martensite. At 40 °C, both phases of sample C were accessible because of the hysteresis loop (Table I), permitting a direct comparison of the reactivity of the two phases. The phase of the NiTi was set by heating or cooling the sample before each immersion into the reactant solution. X-ray powder diffraction verified that preheating or precooling sample C sets the desired phase. The reaction rate for the austenite was 2600 ± 150 Å/s and that for the martensite was 2500 ± 150 Å/s, identical within the error of the measurement.

The apparent activation energies for the bromine reaction with the austenite and martensite were also determined. The kinetic measurements were performed at 10 °C increments at temperatures between 20 and 60 °C, with preheating and precooling each of three NiTi samples, for a total of six extracted apparent activation energies. The results of the experiments are shown in Figure 5. Sample A ($A_s = 6$ °C, $A_t = 20$ °C) is in the austenite phase between 20 and 60 °C, regardless of any previous heating or cooling. Sample C ($A_s = 50$ °C, $M_s = 30$ °C), could be reacted within the test temperature range as either the austenite, if preheated, or martensite phase, if precooled, except for the extreme points, at 60 °C, when precooled and 20 °C, when preheated. Sample B ($A_s = 18$ °C, $M_s < 18$ °C), was either in the austenite phase, if heated before reacting, or in a mixture of phases, if cooled before reacting.

As shown in Figure 5, however, the crystal structure of the NiTi during reaction did not seem to have a measurable effect on the apparent activation energy. Since the variation in the apparent activation energies for the four samples in the austenite phase spans a range from 12 to 16 kJ/mol, with error bars, the values for the martensitic and mixed phase samples are experimentally indistin-

(18) Duerig, T. W.; Wayman, C. M. In *Engineering Aspects of Shape Memory Alloys*; Duerig, T. W., Ed.; Butterworths: London, 1990; p 43.

(19) Hodgeson, D. Shape Memory Applications, Inc., private communication.

(20) Streitwieser, A.; Heathcock, C. H. *Introduction to Organic Chemistry*, 2nd ed.; Macmillan: New York, 1981; p 72.

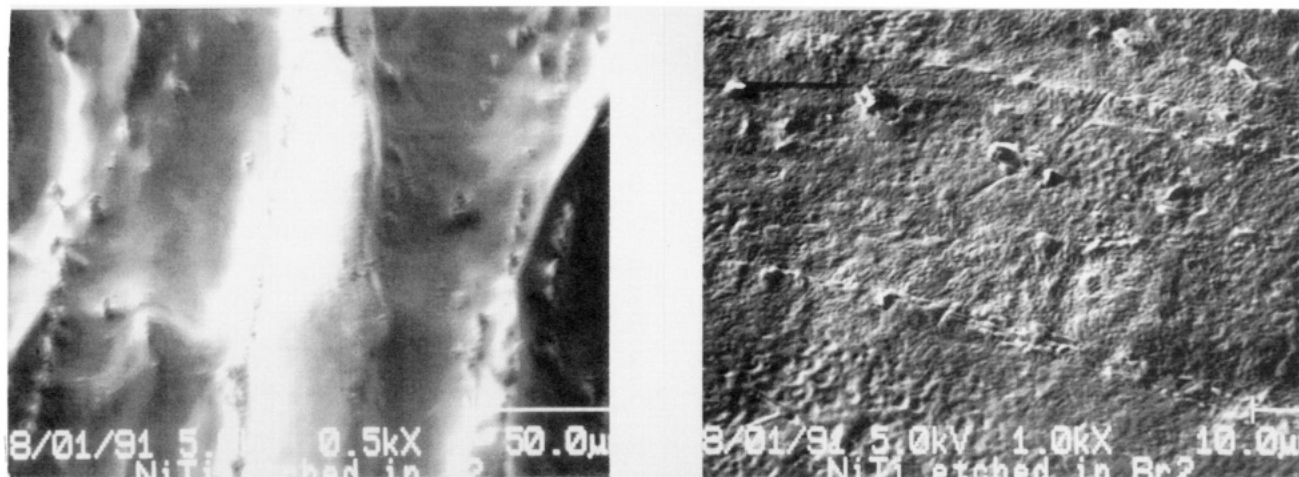


Figure 6. Secondary electron micrographs illustrating the surface morphologies that may be prepared from the corrosion reaction. On the highly textured surface of a sample etched in 1.0 M iodine, at the left, the average size of a surface feature is 50 μm . This is representative of samples etched in low bromine concentrations, as well. The sample on the right, etched in 3.9 M bromine solution, has surface features that are about 1 μm , on average.

guishable from those for the austenite phase, although they both are in the lower part of the range spanned by the austenite data. With sample C, which permits the austenite and martensite apparent activation energies to be compared directly in the same sample, virtually identical results are obtained (Figure 5; "C, heated" vs "C cooled"). Moreover, the Arrhenius plot for a precooled sample of B did not show a change in slope, even though from 20 to 40 $^{\circ}\text{C}$ B is a mixture of phases, and from 40 to 60 $^{\circ}\text{C}$ B is exclusively in the austenite phase. The average activation energy for the NiTi reaction with bromine, including data from all samples, is $13.4 \pm 1.6 \text{ kJ/mol}$.²¹ The lack of selectivity may result from the extreme exothermicity of the reaction.

Surface Morphology. The reaction with bromine is capable of creating a variety of surface finishes on the bulk NiTi solid, depending on concentration. At low concentrations, 0.97 M (5% v/v) Br_2 in MeOH, the NiTi is macroscopically pitted and scarred as a result of the reaction. As the bromine concentration is increased to 3.9 M (20% v/v), the surface is chemically polished, and a mirror finish is created. Samples etched in I_2 , which has limited solubility in MeOH, also show surface relief similar to that seen with low bromine concentrations.

(21) The error bar indicated for the average apparent activation energy was calculated from the standard deviation for the small set of measured apparent activation energies.

Electron micrographs of the surfaces of two NiTi samples, one taken at low I_2 concentration (representative of all the low concentration samples etched in Br_2 and I_2) and one at high Br_2 concentration, are shown in Figure 6. The sample reacted at low I_2 concentration has features that are, on average, about 50 μm large, whereas the sample reacted at high Br_2 concentration has features that are about 1 μm on average. It is unusual to be able to obtain a polished surface of this type without resorting to an electrochemical polishing procedure.

The possibility of selective nickel or titanium etching was explored by taking AES depth profile data of both peaks and troughs of a NiTi sample reacted in 0.97 M bromine solution. The composition of the NiTi was the same in both features, implying that the same amount of nickel and titanium had been removed from each. It may be that Br_2 preferentially attacks grain boundaries or other stressed areas in the sample; more research in this area is needed to address these questions.

Acknowledgment. We acknowledge helpful conversations with Drs. Clark Landis and John Perepezko, the experimental assistance of Ms. Shelly Burnside, Dr. Ngoc Tran, and Mr. John Busch, and financial support from TiNi Alloy Co. and the ONR. We would also like to thank Mr. Chuck Hovey for providing well-characterized NiTi samples with a range of transition temperatures.

Registry No. Br_2 , 7726-95-6; I_2 , 7553-56-2; MeOH, 67-56-1; Ni 47-51, Ti 49-53, 69546-48-1.